Femoral Neck Trabecular Microstructure in Ovariectomized Ewes Treated With Calcitonin: MRI Microscopic Evaluation

Peer-reviewed author version

Jiang, Y.; Zhao, J.; GEUSENS, Piet; Liao, E-Y.; ADRIAENSENS, Peter; GELAN, Jan; Azria, M.; Boonen, S.; Caulin, F.; Lynch, J.A.; Ouyang, X. & Genant, H.K.
(2005) Femoral Neck Trabecular Microstructure in Ovariectomized Ewes Treated With Calcitonin: MRI Microscopic Evaluation. In: JOURNAL OF BONE AND MINERAL RESEARCH, 20(1). p. 125-130.

DOI: 10.1359/JBMR.041008
Handle: http://hdl.handle.net/1942/1008

JOURNAL OF BONE AND MINERAL RESEARCH
Volume 20, Number 1, 2005
Published online on October 18, 2004; doi: 10.1359/JBMR.041008

Femoral Neck Trabecular Microstructure in Ovariectomized Ewes Treated With Calcitonin: MRI Microscopic Evaluation

Yebin Jiang,[1,2] Jenny Zhao,[1] Piet Geusens,[3,4] Er-Yuan Liao,[2] Peter Adriaensens,[3] Jan Gelan,[3] Moïse Azria,[5] Steven Boonen,[6] Francine Caulin,[7] John A Lynch,[1] Xiaolong Ouyang,[1] and Harry K Genant[1]

ABSTRACT: Ovariectomy induces deterioration of the trabecular structure in the femoral neck of ewes, as depicted by MR microscopic imaging. This structural deterioration is prevented by salmon calcitonin treatment.

Introduction: This study evaluated the trabecular (Tb) microarchitecture of an ovariectomy (OVX)-induced osteoporotic model in ewes and determined the effects of salmon calcitonin (sCT), an osteoclast inhibitor, on the Tb structure. This is the first report of OVX-induced changes in the Tb structure in the femoral neck in the ewes and effect of sCT on the microarchitecture.
Materials and Methods: Ewes (5–8 years old, $n = 28$) were equally allocated into sham (Sham), OVX injected with vehicle, or OVX injected with sCT at 50 or 100 IU, three injections per week. They were killed 6 months after OVX. The femoral neck was examined with an MR imager at 9.4 T in axial, coronal, and sagittal planes. An internal calibration procedure as a means of standardizing image analysis was used to adjust the segmentation threshold. Data from all three planes were averaged.
Results and Conclusions: Compared with Sham, OVX induced significant changes ($p < 0.0125$) in the MRI-derived femoral neck Tb structure: Tb bone volume fraction (BV/TV), –18%; Tb number, –20%; Tb separation, +23%; number of free ends, +28%; number of nodes, –39%; number of Tb branches, –23%; mean length of Tb branches, –19%. Compared with OVX, treatment of sCT at 100 IU significantly improved all the Tb structural parameters to the Sham level ($p < 0.0001 \sim p = 0.0281$), whereas 50 IU significantly increased the Tb number and the mean length of the Tb branches. BV/TV explained 74% of the variation of compressive stress of the trabecular cylinder cores of the femoral neck. Combining all structural parameters in a multivariate regression analysis significantly improved the explanation to 84%, and adding BMD further improved the predictive ability of the model to 92%. We conclude that OVX induces deterioration of the MRI-derived Tb microstructure in the femoral neck of ewes. sCT treatment prevents OVX-induced changes. The femoral neck microarchitecture significantly correlates with its biomechanical properties. Combining microstructural parameters with BMD further improves the prediction of bone biomechanical properties. The effects of sCT on OVX ewes may help explain reduced fracture risk in postmenopausal osteoporotic women treated with sCT.
J Bone Miner Res 2005;20:125–130. Published online on October 18, 2004; doi: 10.1359/JBMR.041008

Key words: femoral neck microstructure, biomechanical properties, salmon calcitonin, adult ewe model

INTRODUCTION

Current assessment of osteoporosis, a disease characterized by low bone mass and bone architectural deterioration, consequently increasing the risk of atraumatic fractures,[1] is based on bone densitometry techniques such as QCT and DXA. Although BMD is a widely used method for assessing fracture risk and therapeutic efficacy, it does not always predict the risk of individual fractures or of bone strength, nor does it completely assess the impact of a particular intervention.[2–8] Changes in BMD in the spine and hip during antiresorptive treatment are correlated with reduction of nonvertebral fractures.[9] However, the relation between changes in BMD and reduction of vertebral fractures during therapy is less clear. Clinical trials have shown that the correlation of BMD increases with vertebral fracture risk reduction has proved less consistent than correlation of BMD decreases with greater vertebral fracture risk

Dr Jiang received a grant from Novartis. Dr Azria is an employee of Novartis. Dr Genant is a member of the Novartis Advisory Board. All other authors have no conflict of interest.

[1]Institute of Endocrinology and Metabolism, the Second Xiang-Ya Hospital of Central South University, China; [2]Osteoporosis and Arthritis Research Group, Department of Radiology, University of California, San Francisco, California, USA; [3]Limburgs Universitair Centrum, Diepenbeek, Belgium; [4]Department of Rheumatology, University Hospital, University of Maastricht, Maastricht, The Netherlands; [5]Novartis, Basel, Switzerland; [6]Leuven University Center for Metabolic Bone Diseases and Division of Geriatric Medicine, K.U.Leuven, Leuven, Belgium; [7]F.C. Consulting, Paris, France.

in the untreated. In the Prevent Recurrence of Osteoporotic Fractures (PROOF) study, calcitonin reduced vertebral fracture risk 33% over 5 years, although the increase in spinal BMD was <1.5%. BMD change was statistically significant at years 1 and 2. By the end of the trial, it was 0.6% higher than the placebo group.[10] The Fracture Intervention Trial (FIT) showed that T scores of high-risk women treated with alendronate for 2.9 years rose at the spine, hip, and forearm by 0.5, 0.2, and 0.1 SD, predicting fracture reductions of 25%, 10%, and 5%, respectively, whereas fracture decreases at these sites were 55%, 51%, and 48% greater than seen in controls.[11] A recent reanalysis of the FIT results determined that BMD change from baseline accounted for only 16% of the reduction in vertebral fractures in treated women.[12] The Multiple Outcomes of Raloxifene Evaluation (MORE) trial concluded that only 4% of the 30% decrease in vertebral fractures they observed in raloxifene-treated women was attributable to the 2.6% increase in spinal BMD.[13] Antiresorptive therapy may help maintain trabecular microarchitecture. Thus, the quantitative analysis of trabecular structure may help elucidate the relationships between structural parameters and bone strength.[14–16]

MRI, a complex technology, can clearly delineate trabecular bone because bone mineral lacks free protons and generates no MR signal, whereas adjacent soft tissue and marrow contain abundant free protons and give a strong signal. Using small, highly efficient coils in high-field scanners, MRI can be performed at resolutions sufficient to discriminate individual bone trabeculae.[14] High-resolution MR images that resolve trabecular bone structure can be obtained in vitro at high magnetic field strengths.[14,17–19] We have shown that, with appropriate sequences, it is possible to image trabecular bone in rats in vivo and in vitro.[20,21] In ovariectomized (OVX) rats, MRI shows differences in trabecular bone that are not detected by DXA, which is projectional rather than tomographic, and can not completely eliminate the effects of cortical bone.[20,21] MRI has several advantages in the assessment of bone structure: it gives 3D structure in arbitrary orientations; it is nondestructive, allowing multiple tests on the same sample; and it is noninvasive and nonionizing.

Calcitonin, an osteoclast inhibitor, may also enhance osteoblastic bone formation.[22,23] It inhibits OVX-induced increase of bone resorption in rats.[24,25] We have shown that salmon calcitonin (sCT) preserved BMD measured by DXA and bone strength in trabecular bone of the femoral neck in sheep treated with sCT.[26] In postmenopausal women injected with sCT, the initial sCT study showed clinical efficacy.[27] It prevents trabecular bone loss when given immediately after menopause.[28] Parenterally injected sCT has beneficial effects on bone mass throughout the skeleton, including the proximal femur, at least in patients with established osteoporotic fractures.[29] In early postmenopausal women, sCT, given by nasal spray, inhibits trabecular bone loss without affecting cortical bone loss,[28] indicating that trabecular bone is probably more sensitive to the effect of calcitonin.[30] In a multicenter, randomized, double-blind, placebo-controlled clinical trial, calcitonin has been shown to prevent incident vertebral fracture in osteoporotic postmenopausal women, although its effect on BMD was only modest.[10] Cross-sectional data have even suggested a protective effect on hip fracture incidence.[31]

Our hypothesis is that MRI microscopy will provide additional insight into the trabecular bone microstructure and therefore bone quality of an osteoporotic model in ewes and the response of this model to calcitonin therapy. The specific aims of this study were to evaluate by MRI the trabecular bone microstructure in an OVX-induced osteoporosis model in ewes and to evaluate the effects of treatment on the model with sCT. From these animals, we have reported previously a nonsignificant loss in BMD in the femur after OVX and a significant decrease in biomechanical competence in the trabecular bone cylinder specimen of the femoral neck. Treatment with sCT, at both 50 and 100 IU, resulted in significantly greater compressive stress of the trabecular bone cylinder compared with OVX.[26]

MATERIALS AND METHODS

Animals

Twenty-eight middle-aged (5–8 years old) ewes with a mean body weight of 62 kg were randomly allocated to four groups with seven animals in each group and studied double-blindly: sham OVX injected with a vehicle (Sham), OVX injected with a vehicle (OVX), OVX injected with sCT at 50 IU (OVX + sCT 50), and OVX injected with sCT at 100 IU (OVX + sCT 100). All animals were injected subcutaneously three times per week. Three times per week instead of daily injections were chosen because at the time of the study there was interest in intermittent treatment. They were housed on straw litter, had free access to an automatic drinking trough, and received a daily diet based on hay and a concentrated supplement for each animal of 4 g calcium, 3 g phosphate, 1 g magnesium, 2 g potassium, 1 g sodium, and 300 IU vitamin D_3. All animals were entered in the study within a 4-day period to exclude potential seasonal variations. Operations were performed under fluothame anesthesia. The animals were killed 6 months after operation. The left femoral neck and head were excised, and muscles and fat were removed. The Institutional Committee of Animal Research approved the research protocol.[26]

MR imaging

MR images of the femoral neck and head were obtained in axial, coronal, and sagittal planes, using a spin echo multislice pulse sequence with TR 1 s, TE 1.8 ms, in-plane resolution 78 μ, and slice thickness 1 mm on a Varian Unity 400 NMR instrument at 9.4 T. For image analysis, MR images were transferred to a Sun/SPARC 20 Workstation (Sun Microsystems, Mountain View, CA, USA). The images were processed with in-house semiautomated image processing software tools developed at UCSF[32–34] using AVS (Advanced Visual Systems, Waltham, MA, USA) software interfaces on the workstation.

Imaging processing

The central five slices of the femoral neck were selected for image analysis. The femoral neck was chosen because of

TABLE 1. TRABECULAR MICROSTRUCTURAL CHARACTERISTICS OF THE FEMORAL NECK

		BV/TV (%)	*Tb.N (#/mm²)*	*Tb.Th (μm)*	*Tb.Sp (μm)*	*No. free ends (#/mm²)*	*No. nodes (#/mm²)*	*No. branches (#/mm²)*	*Branch mean length (μm)*
Sham	Mean	25.3	1.98	178	378	6.34	0.447	3.70	190
	SE	0.7	0.04	10	10	0.25	0.030	0.11	9
OVX	Mean	20.7	1.58	171	464	8.14	0.273	2.83	154
	SE	0.7	0.02	8	8	0.39	0.026	0.15	2
	p (vs. Sham)	0.002	<.0001	>0.05	0.0001	0.0051	0.0025	0.0017	0.0056
OVX + CT 50 U	Mean	22.2	1.77	180	426	7.10	0.356	3.07	173
	SE	1.3	0.04	7	20	0.10	0.025	0.11	4
	p (vs. OVX)	0.3823	0.0065	>0.05	0.1500	0.0253	0.0570	0.2549	0.0035
OVX + CT 100 U	Mean	25.9	2.02	178	368	6.51	0.506	3.63	185
	SE	1.7	0.09	8	10	0.14	0.036	0.11	5
	p (vs. OVX)	0.0281	<.0001	>0.05	<.0001	0.0047	0.0007	0.0026	0.0003
p (ANOVA)		0.0337	0.0009	0.897	0.0006	0.0004	0.0003	0.0002	0.0021

its relevance to human osteoporotic hip fracture. An analysis region of interest (ROI) was positioned in the trabecular area of the femoral neck, carefully avoiding the cortical bone and physis, or ossified remnant of the fused growth plate.

An ''internal calibration'' procedure as a means of standardizing the analysis of images obtained at different times and in different samples, which was described in detail previously,[32–34] was used to adjust the threshold value applied to each scan for overall differences in gray-level brightness and contrast. Briefly, the segmentation threshold for each image was determined from the average gray-level values within four ''calibration ROIs,'' that is, two ROIs in cortical bone, yielding low gray-level values, and two ROIs in bone marrow, yielding high gray-level values, on all five contiguous midslices, and the mean gray-level value in each ROI was measured. The segmentation threshold for trabecular bone must separate image pixels representing marrow from those representing bone trabeculae, and therefore, lies somewhere between the high (bright) gray-level values of bone marrow and the low (dark) gray-level values of cortical bone. A single threshold (Th) value was calculated for all five image slices, $Th = Co + \delta(1 - Co/Ma)$, where Co and Ma denote the mean gray value of cortical bone and bone marrow over the five slices, respectively, and δ is an operator-defined empirical constant. The factor $(1 - Co/Ma)$ normalizes the dynamic range of the grayscale in each image. Averaging over all five slices, values greater than the threshold were set to non-bone, and the remaining pixels were set to bone, generating a binary image.

The run-length method[35] was used to calculate the trabecular structure from the binary ROI. Morphological measurements, extrapolated from standard techniques of stereology, were used to derive trabecular bone volume fraction (BV/TV), thickness (Tb.Th), and separation (Tb.Sp). Measurements of trabecular connectivity, including number of trabecular nodes, number of free ends, number of branches, and mean length of the branches were obtained from the skeletonized trabecular network generated by using thinning algorithms.[36] All skeletons possessed the typical properties such as connectedness and one-pixel thickness.

The analysis was performed on MR images of all three axial, coronal, and sagittal planes, and their results were averaged for each specimen. The operators were blinded to treatment for MR images acquisition and analysis.

Statistical analysis

Comparisons among groups were performed using the ANOVA test. In the multiple comparison procedure, $p < 0.0125$ was considered significant after Bonferroni adjustment. Relationships between the biomechanical properties, morphometrical parameters, and BMD were assessed using linear regression analyses. The relationship between a combination of more than one parameter, namely trabecular structural parameters and bone mineral measurements, with the biomechanical properties was studied using multivariate regression analysis. In the multivariate regression analysis, all trabecular structural parameters and bone mineral measurements were added into the model as predictive variables, whereas compressive stress was the outcome variable. The insignificant variables were excluded.

RESULTS

As shown in Table 1 and Fig. 1, OVX induced significant changes in all trabecular microstructural parameters in the femoral neck except trabecular thickness. Compared with OVX, treatment of sCT at 100 IU significantly improved all the trabecular microstructural parameters in the femoral neck except trabecular bone volume fraction and trabecular thickness, whereas at 50 IU, sCT significantly increased the trabecular number and the mean length of the trabecular branches.

Trabecular bone volume fraction explained 74% of the variance in compressive stress (Fig. 2). Combining all structural parameters significantly improved the predictive ability to 84%, and adding BMD further improved the proportion explained by the model to 92%. Trabecular bone volume fraction moderately correlated with biomechanical parameters, whereas all other trabecular microstructural parameters modestly related with the results of the biomechanical testing (Table 2).

No significant differences between groups were found in serum calcium, phosphate, alkaline phosphatase, calcitonin, and osteocalcin (data not shown).

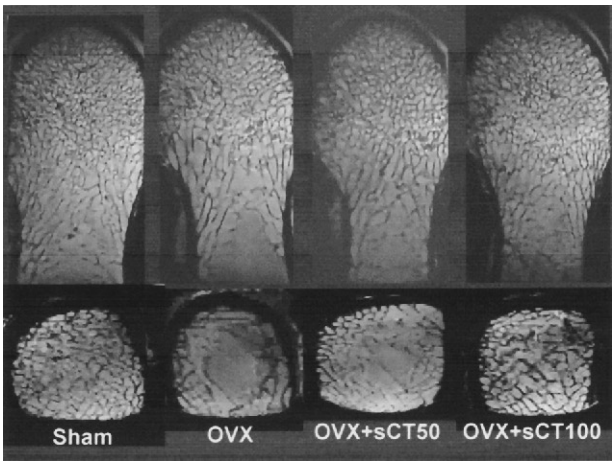

FIG. 1. MR microscopic images of the femoral neck and head show that the OVX-induced loss in trabecular microstructure in the femoral neck is prevented by the treatment of sCT.

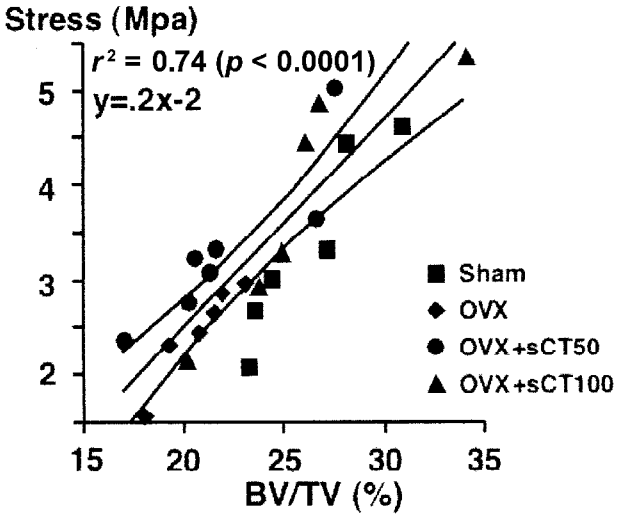

FIG. 2. Relationship between trabecular bone volume fraction and compressive stress in the femoral neck.

DISCUSSION

In this study, we quantified OVX induced loss of the trabecular microstructure by 3D MR microscopic imaging of the femoral neck of the ewes. These OVX-induced changes in trabecular microstructure were prevented by sCT treatment. This is the first report of MRI-derived Tb microarchitectural deterioration in the femoral neck induced by OVX and protective effects of sCT on the microstructure in the ewes.

Preservation of the trabecular microstructure in the femoral neck of the estrogen-deprived ewes by sCT is not unexpected, in view of the clinical studies of sCT in osteoporosis.[10,27,28,30,37] Our data are also in agreement with other preclinical observations. In addition to its inhibitory effects on osteoclastic bone resorption, calcitonin may enhance osteoblastic bone formation.[22,23] Studies in OVX rats using traditional 2D bone histomorphometry have shown that subcutaneous administration of calcitonin is associated with a partial inhibition of the OVX-induced increase in bone resorption, without detriment effects on osteoid volume or mineralization lag time.[24,25] In young adult rats, 3 U/kg subcutaneously for 40 days did not show detrimental effects on femoral torsional mechanical properties,[38] whereas adult beagles treated with calcitonin at 8 mg/kg/day for one-half of a year had a significant decrease in the whole lumber vertebra (L_2) strength.[39] The latter discrepant result remains enigmatic and unexplained. In the adult OVX ewe model, we have previously reported the positive effect of long-term intermittent administration of sCT on femoral cortical and trabecular bone strength.[26] To this end, torsional and compressive tests as well as resonant frequency analysis were performed. After treatment with sCT, compressive stress was found to be preserved in the trabecular cylinder core of the femoral neck. Because the relation between the mineral and the organic matrix may contribute to bone biomechanical properties, crystallographic parameters and crystal size and/or perfection were measured by powder X-ray diffractometry to assess the chemical stability and the mechanical strength of the bone mineral. We found no changes in diffraction pattern and no effect of OVX or sCT treatment on crystal size or perfection parameters.[26] These results were in line with prior histomorphometric reports, showing no deleterious effect of subcutaneously injected calcitonin on bone mineralization in humans.[40,41] They may point to a difference between sCT and other inhibitors of bone resorption, such as bisphosphonates, which bind strongly to hydroxyapatite crystals and potentially may inhibit crystal formation and dissolution.[42]

The changes in the femoral neck trabecular microstructure after OVX and sCT treatment are more sensitively assessed than the changes in the bone mineral measurements using both DXA and dual energy quantitative CT (DEQCT).[26] In a human study, no significant difference was found in pQCT trabecular BMD at the distal radius in vivo between premenopausal and postmenopausal women, but the number of trabecular perforations significantly increased in postmenopausal compared with premenopausal women. These results indicate that increased disconnectivity may occur without a significant reduction of BMD and that trabecular bone connectivity is more sensitive than BMD in the detection of the early changes of postmenopausal osteoporosis.[43]

The findings in this study can be explained by several arguments. MR microscopic imaging has very high resolution, allowing pinpoint evaluation of the trabecular structure of the secondary spongiosa of the femoral neck. The sensitivity of DEQCT could be compromised because of relatively large field of view (FOV) and small specimen, which would result in partial volume average of both trabecular and cortical bone at the endocortical junction, masking of purely trabecular bone changes. In addition, the bone in the epiphysis, physis, and primary spongiosa usually changes little in response to estrogen deprivation,[19] and these regions might be included in the measurement ROI because of partial volume average in the DEQCT examination. Similarly, the DXA examination of the cylinder core might also include the epiphysis, physis, and primary spongiosa. Finally, Table 2 shows that, among correlation

Table 2. Correlation Coefficients Between Trabecular Microstructural Parameter, Biomechanical Testing, and DEQCT and DXA Examination of the Femoral Neck

	BV/TV	*Tb.N*	*Tb.Th*	*Tb.Sp*	*No. free ends*	*No. nodes*	*No. branches*	*Branch mean length*
Stress	0.86*	0.73*	–0.09	–0.25*	–0.26*	0.55*	0.63*	0.52*
Stiffness	0.79*	0.65*	–0.01	–0.15	–0.16	0.46*	0.58*	0.41*
Strain	0.58*	0.60*	–0.12	–0.46*	–0.38*	0.48*	0.59*	0.70*
DEQCT	0.64*	0.45*	–0.04	–0.07	–0.06	0.28*	0.47*	0.22*
DXA BMD	0.75*	0.57*	0.01	–0.11	–0.17	0.39*	0.57*	0.37*
BV/TV		0.90*	–0.29*	–0.37*	–0.34*	0.66*	0.67*	0.50*
Tb.N			0.19	–0.58*	–0.55*	0.74*	0.77*	0.56*
Tb.Th				–0.24*	–0.11	0.08	–0.13	–0.07
Tb.Sp					0.47*	–0.65*	–0.48*	–0.54*
No. free ends						–0.70*	–0.70*	–0.58*
No. nodes							0.67*	0.68*
No. branches								0.68*

* $p < 0.05$.

coefficients between trabecular microstructural parameters and BMD of both DEQCT and DXA examination, bone volume fraction has highest correlation. After Bonferroni correction in the multiple comparison procedure, the increase of bone volume fraction in the sCT-treated animals is no longer statistically significant. The discrepancy of lack of significant changes in bone volume fraction and in BMD but significant changes in biomechanical properties in the femoral neck trabecular bone after sCT treatment in this study is in agreement with modest change in BMD but significant reduction in vertebral fracture rate observed in clinical trial.[10]

Our finding that a combination of microstructural parameters with bone mineral measurements provided the best prediction of bone strength is in line with our earlier work predicting the mechanical properties of trabecular bone cubes from human vertebral bodies.[33] Previous studies have reported modest correlations between trabecular structural parameters as assessed by CT and BMD of the lumbar vertebrae.[44] Similarly, modest correlations have been reported in a study of MRI-assessed trabecular structure and CT-determined BMD.[45] Our study, along with previous other reports,[33,44,46–48] support the concept that structural analysis provides an additional tool to analyze bone quality of trabecular bone. Further studies are warranted to investigate the microstructure and biomechanical properties of the cortical bone after antiresorptive therapy.

In summary, OVX induces a deterioration of the trabecular microstructure in the femoral neck of the adult ewe. These OVX-induced changes in trabecular microstructure and biomechanical properties are prevented by the administration of sCT. The effects of sCT as observed in this animal model may help explain the reduction in fracture risk in postmenopausal osteoporotic women treated with sCT.

ACKNOWLEDGMENTS

This study was supported in part by Novartis.

REFERENCES

1. Conference Report 1991 Consensus development conference: Prophylaxis and treatment of osteoporosis. Osteoporosis Int **1:**114–117.
2. McBroom RJ, Hayes WC, Edwards WT, Goldberg RP, White AA 1985 Prediction of vertebral body compression fracture using quantitative computed tomography. J Bone Joint Surg Am **67:**1206–1214.
3. Dempster DW, Ferguson PM, Mellish RW, Cochran DV, Xie F, Fey C, Horbert W, Parisien M, Lindsay R 1993 Relationships between bone structure in the iliac crest and bone structure and strength in the lumbar spine. Osteoporos Int **3:**90–96.
4. Genant HK, Gordon C, Jiang Y, Lang TF, Link TM, Majumdar S 1999 Advanced imaging of bone macro and micro structure. Bone **25:**149–152.
5. Jiang Y, Zhao J, Van Audekercke R, Dequeker J, Geusens P 1996 Effects of low-dose long-term NaF preventive treatment on rat bone mass and biomechanical properties. Calcif Tissue Int **58:**30–39.
6. Jiang Y, Zhao J, Van Audekercke R, Dequeker J, Geusens P 1997 Long-term effects of naproxen on bone mass and biomechanic properties of the femur and vertebral body of ovariectomized rats on normal or low calcium diet. J Bone Miner Res **19:**820–831.
7. Jiang Y, Zhao J, Rosen C, Geusens P, Genant HK 1999 Perspectives on bone mechanical properties and adaptive response to mechanical challenge. J Clin Densitometry **2:**423–433.
8. Geusens P 1992 Photon Absorptiometry in Osteoporosis: Bone Mineral Measurements in Animal Models and in Humans. Orientaliste, Leuven, Belgium.
9. Hochberg MC, Greenspan S, Wasnich RD, Miller P, Thompson DE, Ross PD 2002 Changes in bone density and turnover explain the reductions in incidence of nonvertebral fractures that occur during treatment with antiresorptive agents. J Clin Endocrinol Metab **87:**1586–1592.
10. Chesnut CH, Silverman S, Andriano K, Genant HK, Gimona A, Harris S, Kiel D, LeBoff M, Maricic M, Miller P, Moniz C, Peacock M, Richardson P, Watts N, Baylink D 2000 A randomized trial of nasal spray salmon calcitonin in postmenopausal women with established osteoporosis: The prevent recurrence of osteoporotic fractures study. Am J Med **109:**267–276.
11. Black DM, Thompson DE, Bauer DC, Ensrud K, Musliner T, Hochberg MC, Nevitt MC, Suryawanshi S, Cummings SR 2000 Fracture risk reduction with alendronate in women with osteoporosis: The Fracture Intervention Trial. J Clin Endocrinol Metab **85:**4118–4124.
12. Cummings SR, Karpf DB, Harris F, Genant HK, Ensrud K, LaCroix AZ, Black DM 2002 Improvement in spine bone density and reduction in risk of vertebral fractures during treatment with antiresorptive drugs. Am J Med **112:**281–289.
13. Sarkar S, Mitlak BH, Wong M, Stock JL, Black DM, Harper KD 2002 Relationships between bone mineral density and in-

cident vertebral fracture risk with raloxifene therapy. J Bone Miner Res **17:**1–10.
14. Chung H, Wehrili FW, Williams JL, Kugelmass SD 1993 Relationship between NMR transverse relaxation, trabecular bone architecture, and strength. Proc Natl Acad Sci USA **90:**10250–10254.
15. Jiang Y, Zhao J, Genant HK 2002 Macro and micro imaging of bone architecture. In: Bilezikian JP, Raisz LG, Rodan GA (eds.) Principles of Bone Biology, 2nd ed. Academic Press, San Diego, CA, USA, pp. 1599–1623.
16. Jiang Y, Zhao J, Mitlak BH, Wang O, Genant HK, Eriksen EF 2003 Recombinant human parathyroid hormone (1–34) (teriparatide) improves both cortical and cancellous bone structure. J Bone Miner Res **18:**1932–1941.
17. Majumdar S, Newitt D, Jergas M, Gies A, Chiu E, Osman D, Keltner J, Keyak J, Genant HK 1995 Evaluation of technical factors affecting the quantification of trabecular bone structure sing magnetic resonance imaging. Bone **17:**417–430.
18. Hipp JA, Jansujwicz A, Simmons CA, Snyder B 1996 Trabecular bone morphology using micro-manetic resonance imaging. J Bone Miner Res **11:**286–297.
19. Jiang Y 1995 Radiology and Histology in the Assessment of Bone Quality. Peeters & Jiang, Leuven, Belgium.
20. White DL, Schmidlin O, Jiang Y, Zhao J, Majumdar S, Genant HK, Morris RC Jr 1997 MRI of Trabecular Bone in an Ovariectomized Rat Model of Osteoporosis. International Society for Mangetic Rosonance in Medicine, Vancouver, Canada.
21. Jiang Y, Zhao J, White DL, Genant HK 2000 Micro CT and micro MR imaging of 3D architecture of animal skeleton. J Musculoskel Neuron Interact **1:**45–51.
22. Farley JR, Tarbaux NM, Hall SL, Linkhart TA, Baylink DJ 1988 The antibone resorptive agent calcitonin also acts in vitro to directly increase bone formation and bone cell proliferation. Endocrinology **123:**159–167.
23. Farley JR, Wergedal JE, Hall SL, Herring S, Tarbaux NM 1991 Calcitonin has direct effects on 3 [H] Thymidine incorporation and alkaline phosphatase activity in human osteoblast-line cells. Calcif Tissue Int **48:**297–301.
24. Hayashi T, Yamamuro T, Okumura H, Kasai R, Tada K 1989 Effect of (Asu1,7)-eel calcitonin on the prevention of osteoporosis in-duced by combination of immobilization and ovariectomy in the rat. Bone **10:**25–28.
25. Wronski TJ, Yen CF, Burton KW, Mehta RC, Newman PS, Soltis EE, DeLuca PP 1991 Skeletal effects of calcitonin in ovarectomized rats. Endocrinology **129:**2246–2250.
26. Geusens P, Boonen S, Nijs J, Jiang Y, Lowet G, Van Audekercke R, Huyghe C, Caulin F, Very JM, Dequeker J, Van der Perre G 1996 Effects of salmon calcitonin on femoral bone quality in adult ovariectomized ewes. Calcif Tissue Int **59:**315–320.
27. Gruber HE, Ivey JL, Baylink DJ, Matthews M, Nelp WB, Sisom K, Chesnut CH 1984 Long-term calcitonin therapy in postmenopausal osteoporosis. Metabolism **33:**295–303.
28. Overgaard KY 1994 Effect of intranasal calcitonin therapy on bone mass and bone turnover in early postmenopausal women: A dose response study. Calcif Tissue Int **55:**82–86.
29. Civitelli R, Gonnelli S, Zachei F, Bigazzi S, Vattimo A, Avioli LV, Gennari C 1988 Bone turnover in postmenopausal osteoporosis. Effect of calcitonin treatment. J Clin Invest **82:**1268–1274.
30. Chesnut CH 1995 Drug therapy; calcitonin, bisphosphonates, and anabolic steroids. In: Riggs BL, Melton LJ (eds.) Osteoporosis: Etiology, Diagnosis and Management. Lippincott-Raven Publishers, Philadelphia, PA, USA.
31. Kanis JA, Johnell O, Gullberg B, Allander E, Dilsen G, Gennari C, Lopes Vaz AA, Lyritis GP, Mazzuoli G, Miravet L 1992 Evidence for the efficacy of bone active drugs in the prevention of hip fracture. BMJ **305:**1124–1128.
32. Ouyang X, Selby K, Lang P, Engelke K, Klifa C, Fan B, Zucconi F, Hottya G, Chen M, Majumdar S, Genant HK 1997 High resolution magnetic resonance imaging of the calcaneus: Age-related changes in trabecular structure and comparison with dual X-ray absorptiometry measurements. Calcif Tissue Int **60:**139–147.
33. Jiang Y, Zhao J, Augat P, Ouyang X, Lu Y, Majumdar S, Genant HK 1998 Trabecular bone mineral and calculated structure of human bone specimens scanned by peripheral quantitative computed tomography: Relation to biomechanical properties. J Bone Miner Res **13:**1783–1790.
34. Jiang Y, Zhao J, van Holsbeeck M, Flynn MJ, Ouyang X, Genant HK 2002 Trabecular microstructure and surface changes in the greater tuberosity in rotator cuff tears. Skeletal Radiol **31:**522–528.
35. Durand E, Ruegsegger P 1991 Cancellous bone structure: Analysis of high-resolution CT images with the run-length method. J Comput Assist Tomogr **15:**133–139.
36. Korstjens CM, Geraets WG, van Ginkel FC, Prahl-Andersen B, van der Stelt PF, Burger EH 1995 Longitudinal analysis of radiographic trabecular pattern by image processing. Bone **17:**527–532.
37. Overgaard K, Hansen MA, Jensen B, Christiansen C 1992 Effect of calcitonin given intranasally on bone mass and fracture-rates in established osteoporosis: A dose-response study. BMJ **305:**556–561.
38. Ekeland A, Myhre L, Underdale T 1983 Effects of salmon calcitonin on mechanical properties of healing and intact bone and skin in rats. Acta Orthop Scand **54:**462–469.
39. Goldstein SA, Goulet R, McCubbrey D 1993 Measurement and significance of three-dimensional architecture to mechanical integrity of trabecular bone. Calcif Tissue Int **53:**S127–S133.
40. Palmieri GMA, Pitcock JA, Brown P, Karas JG, Roen LJ 1989 Effect of calcitonin and vitamin D in osteoporosis. Calcif Tissue Int **45:**137–141.
41. Kroger H, Arnala I, Alhava EM 1992 Effect of calcitonin on bone histomorphometry and bone metabolism in rheumatoid arthritis. Calcif Tissue Int **50:**11–13.
42. Grynpass MD, Acito A, Dimitriu M, Mertz BP, Very JM 1992 Changes in bone mineralization, architecture and mechanical properties due to long-term (1 year) administration of pamidronate (APD) to adult dogs. Osteoporos Int **2:**74–81.
43. Takagi Y, Fujii Y, Miyauchi A, Goto B, Takahashi K, Fujita T 1995 Transmenopausal change of trabecular bone density and structural pattern assessed by peripheral quantitative computed tomography in Japanese women. J Bone Miner Res **10:**1830–1834.
44. Chevalier F, Laval-Jeantet A, Laval-Jeantet M, Bergot C 1992 CT image analysis of the vertebral trabecular network in vivo. Calcif Tissue Int **51:**8–13.
45. Majumdar S, Genant HK, Grampp S, Newitt DC, Truong VH, Lin JC, Mathur A 1997 Correlation of trabecular bone structure with age, bone mineral density, and osteoporotic status: In vivo studies in the distal radius using high resolution magnetic resonance imaging. J Bone Miner Res **12:**111–118.
46. Carter DR, Hayes WC 1977 The compressive behavior of bone as a two-phase porous structure. J Bone Joint Surg Am **59A:**954–962.
47. Vesterby A, Mosekilde L, Gundersen HJ, Melsen F, Mosekilde L, Holme K, Sorensen S 1991 Biologically meaningful determinants of the in vitro strength of lumbar vertebrae. Bone **12:**219–224.
48. Dalstra M, Huiskes A, Odgaard EV 1993 Mechanical and textural properties of pelvic trabecular bone. J Biomech **27:**375.

Address reprint requests to:
Yebin Jiang, MD, PhD
Osteoporosis and Arthritis Research Group
Department of Radiology
University of California
San Francisco, CA 94143-0628, USA
E-mail: Yebin.Jiang@radiology.ucsf.edu

Received in original form February 26, 2004; revised form July 29, 2004; accepted August 12, 2004.